Available online at www.sciencedirect.com
ScienceDirect
Physics of the Earth and Planetary Interiors 164 (2007) 186–196
PHYSICS OF THE EARTH AND PLANETARY INTERIORS
www.elsevier.com/locate/pepi

Effects of solute segregation on the grain-growth kinetics of orthopyroxene with implications for the deformation of the upper mantle

Philip Skemer*, Shun-ichiro Karato

Department of Geology and Geophysics, Yale University, P.O. Box 208109, New Haven, CT 06520-8109, USA

Received 19 March 2007; received in revised form 9 June 2007; accepted 29 June 2007

Abstract

The kinetics of static grain growth in a pure synthetic orthopyroxene and orthopyroxene of natural composition were investigated to determine the effects of solute segregation on grain growth. In all experiments the grain size of the synthetic orthopyroxene increases considerably; in contrast, the natural orthopyroxene shows no perceptible grain growth at the same conditions. High-resolution X-ray compositional mapping confirms that the natural orthopyroxene has large concentrations of aluminum and calcium cations segregated on and near its grain boundaries. This segregation is believed to be responsible for the slow grain-growth kinetics in the natural orthopyroxene. Slow grain growth may permit long-term deformation in the diffusion creep regime, as has been observed in some deep mantle xenoliths. As such, it may provide a means of weakening the lithosphere.

Keywords: Orthopyroxene; Grain growth; Impurity drag; Shear localization

1. Introduction

Orthopyroxene is the second most abundant mineral throughout much of the upper mantle, however its rheological properties are poorly understood from an experimental perspective. A frequent assumption made in the study of the upper mantle is that the aggregate rheology is primarily controlled by the rheology of olivine (e.g., Karato and Wu, 1993). However, observations from some deep mantle xenoliths suggest that at certain conditions orthopyroxene may also play a significant role in deformation. Unlike most shallow peridotites, these xenoliths contain microstructural evidence for grain-size reduction and subsequent grain-size sensitive deformation of orthopyroxene, coupled with grain-size insensitive deformation of olivine (Boullier and Gueguen, 1975). The orthopyroxene, in addition to deforming by a grain-size sensitive mechanism, becomes interconnected at high strains, suggesting that its rheology may contribute significantly to the rheology of the aggregate material (Handy, 1994). Grain-size sensitive deformation is of particular interest, because it is thought to be an important mechanism for shear localization (e.g., Rutter and Brodie, 1988; Bercovici and Karato, 2002). Shear localization is, in turn, believed to be essential for the formation of tectonic plates (e.g., Bercovici, 2003). Thus, long-term deformation by orthopyroxene in a grain-size sensitive regime may, under some circumstances, play a key role in the evolution of plate tectonics.

Grain size is not an equilibrium quantity, but rather a continuously varying property that results from the

* Corresponding author. Tel.: +1 203 432 5791; fax: +1 203 432 3134.
E-mail address: philip.skemer@yale.edu (P. Skemer).

0031-9201/$ – see front matter © 2007 Elsevier B.V. All rights reserved.
doi:10.1016/j.pepi.2007.06.011

competition between grain-growth and grain-size reducing processes. In order for grain-size sensitive creep to dominate deformation over a geological time scale, the recrystallized grain size must be small, and the kinetics of grain growth must be slow (de Bresser et al., 1998, 2001). In this study we focus specifically on this latter issue. The kinetics of grain growth have been studied for a number of Earth materials (e.g., Tullis and Yund, 1982; Karato, 1989; Dresen et al., 1996; Nishihara et al., 2006). Additionally, it has long been recognized that grain growth is inhibited by the presence of dissolved impurities segregated to grain-boundaries and near-grain-boundary regions (e.g., Yan et al., 1977). This effect, known as impurity drag, has been recognized in halite (Guillopé and Poirier, 1979), olivine (Toriumi, 1982), and calcite (Covey-Crump, 1997). However, there have been no experimental studies on these processes in orthopyroxene. In this study we report the first data on the grain-growth kinetics in orthopyroxene. We will demonstrate that certain cations, dissolved on and near-grain boundaries, play a crucial role in controlling the kinetics of grain growth in orthopyroxene, and as such may have important consequences for the rheology of the mantle.

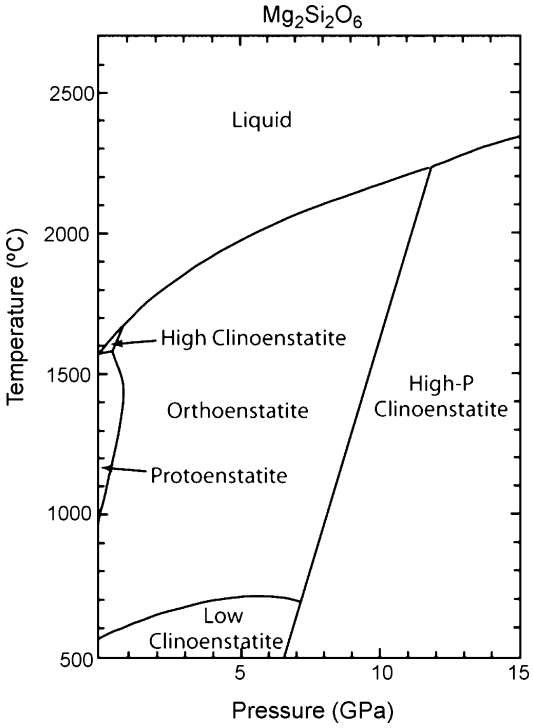

Fig. 1. Phase diagram for $Mg_2Si_2O_6$ after Presnall (1995). The stable phase in most of the upper mantle is orthoenstatite, which requires experiments to be conducted at $P > 1$ GPa.

2. Methods

A complicating factor in the study of orthopyroxene is that it has a number of polymorphs at low pressure (Fig. 1). To study its properties in the appropriate stability field for most of the upper mantle – orthoenstatite – experiments must be done at modest pressures. This precludes study using room-pressure furnaces and in most gas-medium apparatuses. Thus, all experiments in this study were conducted in a solid medium apparatus.

To study the effects of solute segregation on the kinetics of grain growth in orthopyroxene, experiments were conducted on two different starting materials. The first starting material was a pure, synthetic orthopyroxene with a nominal formula of $Mg_{1.8}Fe_{0.2}Si_2O_6$ (henceforth synthetic orthopyroxene). The preparation of the synthetic orthopyroxene involved several steps. First $(Mg_{0.9}Fe_{0.1})O$ powder was synthesized from MgO and Fe_2O_3 powders with purity >99.95%. The powders were dried at 400 K in a vacuum furnace to remove adsorbed water, weighed, and mechanically mixed before being cold-pressed into ~1 cm^3 cylindrical pellets. The pellets were placed in a 1 atm furnace for 24 h at 1473 K with the oxygen fugacity ($f_{O_2} = 10^{-5}$ Pa) buffered using a continuously running mixture of CO and CO_2. The run product was recovered, ground in a Syalon^{TM} ball-mill, cold-pressed into new pellets, and reacted again at the same conditions. Mixing and reacting the sample twice helped ensure the completeness of the reaction. The $(Mg_{0.9}Fe_{0.1})O$ powder was then mixed with SiO_2 powder (with purity >99.995%), which was calcined at 1273 K for 2 h to remove adsorbed water immediately prior to mixing. This powder then went through two cycles of cold pressing, annealing at high temperature (at 1 atm and 1473 K, for 24 h), and grinding. The powder was examined optically and with Raman spectroscopy to determine the completeness of the reaction. A second starting material was produced from large (1–2 mm), optically clear orthopyroxene crystals hand selected from the San Carlos peridotite (henceforth natural orthopyroxene). In both cases, fine-grained powders were produced by grinding the starting materials under distilled water in a Syalon^{TM} ball-mill for several hours. Further grain-size refinement was achieved by gravitationally settling the powders in distilled water. Once all grains >3 μm were removed, the powder was dried overnight at 400 K in a vacuum furnace before being loaded into a nickel capsule. The powder samples were isostatically hot pressed at 1.5 GPa, 1273 K, for 1 h (synthetic orthopyroxene) or at 1.5 GPa, 1473 K, for 3 h (natural orthopyroxene) in a Griggs-type solid medium apparatus. The intention of these hot-pressing experiments was to produce fine-grained, dense, polycrystalline aggregates. The synthetic orthopyroxene was hot pressed at a lower temperature to minimize any initial

Table 1
Composition of starting materials

	Synthetic orthopyroxene	Natural orthopyroxene
Al_2O_3	†	3.10
SiO_2	58.27	55.67
CaO	†	0.78
FeO	7.05	5.65
K_2O	–	–
TiO_2	–	–
MnO	–	0.16
Na_2O	–	†
MgO	33.37	33.17
Total	98.69	98.53

(–): not detected; (†): detected, but not quantifiable.

grain growth. For the natural orthopyroxene powder samples, it was necessary to hot press at a higher temperature to obtain sufficiently dense samples. After recovering the samples, the run products were examined optically, with Raman spectroscopy, and with electron microprobe analysis, to confirm the composition (Table 1).

Grain-growth experiments were conducted with both starting materials in the same capsule so properties could be directly compared at identical experimental conditions. All experiments were conducted at 1.5 GPa and 1473–1573 K. Experiments were not run at higher temperatures to avoid the generation of melt. For each experiment, a half-disk of each starting material was loaded into a capsule machined from nickel with purity >99.99% (Fig. 2). The solid nickel capsule was used to buffer the oxygen fugacity, as well as minimize any differential stress transferred to the sample from the assembly. A small amount of olivine powder was added to buffer the oxide activity. The assembly was compressed over 3 h at room temperature to the target pressure. The temperature was then increased to the desired level at 20 K/min. The temperature and the thermal gradient were monitored using Pt-Pt13%Rh thermocouples placed at the middle and the bottom of the capsule. The samples were annealed for 4–34 h. At the conclusion of the experiment, temperature was quenched by shutting off the power to the furnace and the pressure was reduced slowly to prevent the formation of decompression cracks. The sample was recovered, mounted in low-viscosity resin, and polished for analysis using a slurry of colloidal silica.

No water was intentionally added to the samples during the synthesis process or during the grain-growth experiments. However, it is often observed that some water can be incorporated into the sample during certain parts of the experimental procedure (e.g., Nishihara et al., 2006). Therefore, the amount of water present in the crystal lattice of both the starting materials and the products of the grain-growth experiments was measured using Fourier transform infrared spectroscopy (FTIR). FTIR measurements were made with an unpolarized beam on doubly polished polycrystalline samples placed on KBr mounting disks. The samples measured were typically 100–150 μm thick. Analyses were made on crack-free regions of the sample with an aperture-limited spot-size of 100 μm × 100 μm. Several measurements were made for each sample, and water contents were estimated using the calibration of Paterson (1982).

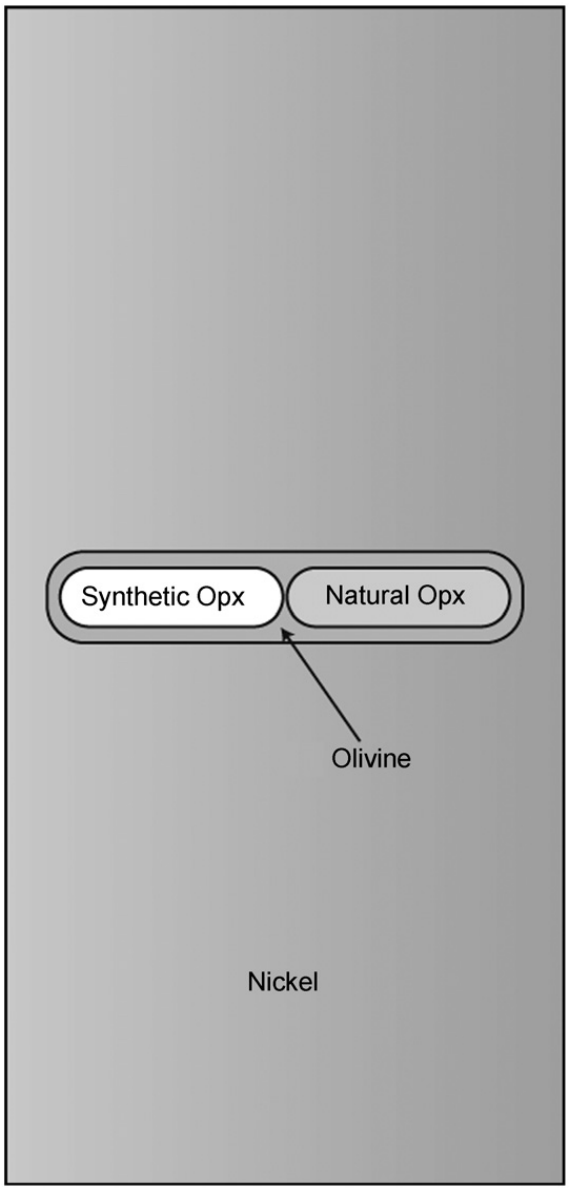

Fig. 2. Cell assembly for the grain-growth experiments. Small pieces of synthetic and natural orthopyroxene were placed adjacent to one another, surrounded by olivine powder, in a solid nickel tube, 4 mm in diameter and 10.7 mm in length.

The average grain size was determined for both the starting hot-pressed samples and for the products of the

grain-growth experiments. Grain sizes were measured on images taken using a scanning electron microscope (SEM) in secondary electron mode. Grain boundaries were illuminated by etching the sample with a colloidal silica suspension, and by rotating the stage of the SEM by 70° to generate shadows. The grain-size measurement was made using the mean lineal intercept technique with a sectioning correction factor of 1.5. Approximately 10 regions were measured for each sample to account for any spatial variation in grain size. The total number of grains measured for each sample typically exceeded 500. Porosity was measured from the secondary electron images by processing the image with a threshold function and comparing the number of pixels from grains and from pores. Grain shape and size for some samples was determined by digitally tracing individual grain boundaries, and then fitting an ellipse to each grain. These data were then used to calculate grain-size distributions using the Schwartz-Saltykov method to correct for the sectioning effect (Underwood, 1970).

The primary source of uncertainty in these experiments is the grain-size measurement, which may vary by up to 20% from region to region within a sample. The temperature measurement is estimated to be accurate to within ±10 K, based on the observed variation in the thermocouple reading. The uncertainty in the pressure measurement is estimated to be less than 10% (Mirwald et al., 1975).

3. Results

The grain morphology and the contrast in grain growth between the synthetic and natural orthopyroxene is illustrated in Fig. 3. In general the shape of the grains is somewhat elongated, but rarely exceeds an aspect ratio of 3:1. The synthetic orthopyroxene starting material has a mean grain aspect ratio of about 2, but a typical run product has mean grain aspect ratios of 1.5. No melt was optically detectable in these experiments. In both the starting materials and the run products, very little water (∼50 ppm H/Si) was detected by FTIR, so

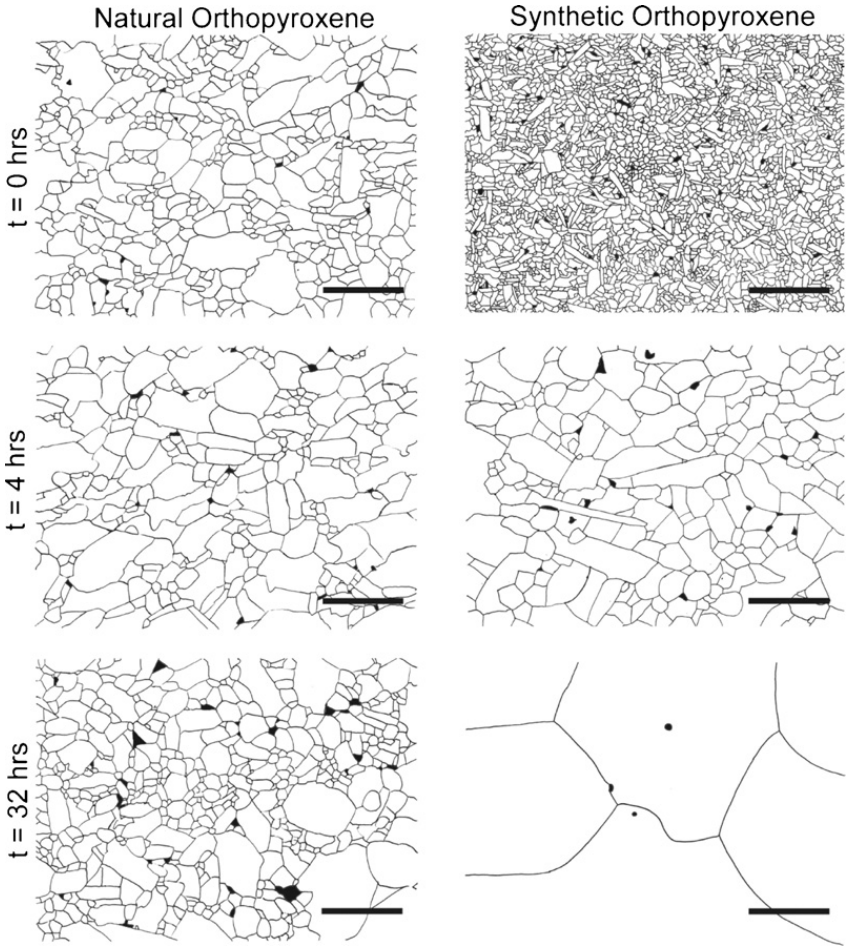

Fig. 3. Grain-size evolution in natural and synthetic orthopyroxene. While the natural orthopyroxene shows no perceptible grain growth, the mean grain size increases dramatically in the synthetic orthopyroxene. All experiments shown here were conducted at 1.5 GPa and 1573 K, under dry conditions. The scale bar is 10 μm. Black regions represent remnant porosity, or grains that were removed during polishing.

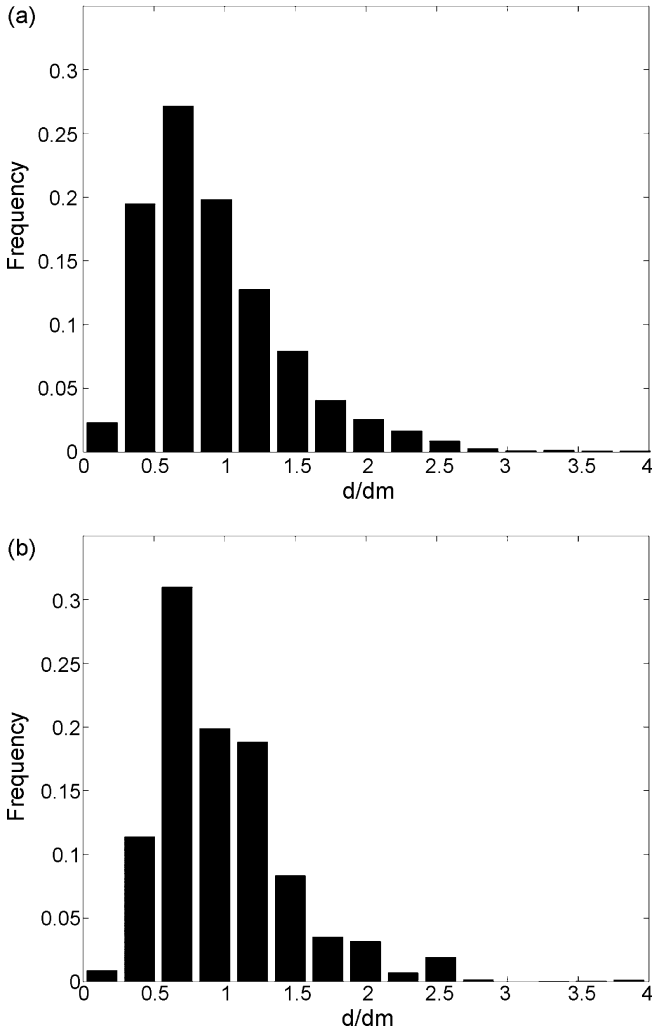

Fig. 4. Grain-size distribution for (a) the synthetic starting material and (b) grain-growth experiment GA-152. Frequency is plotted as a function of d/d*m*, which is the grain size normalized by the mean grain size. These distributions are corrected for the two-dimension sectioning effect using the Schwartz-Saltykov method. There is little change in the peak location and the broadness of the distribution, indicating that grain growth occurred by normal processes.

these experiments are considered to be dry. There is little change in the shape or broadness of the normalized grain-size distribution as a function of time (Fig. 4), indicating that grain growth occurred by "normal" processes (Hillert, 1965; Atkinson, 1988). Complete densification was not generally achieved in these experiments; some remnant porosity was always present. In the synthetic starting material, which was hot pressed for a short time to avoid the initiation of grain growth, porosity was as high as 5%. However during the first few hours of the grain-growth experiments, porosity dropped to <1% and remained constant at this level. This level of porosity is comparable in both the natural and the synthetic samples. Porosity is known to have a substantial effect on grain-growth kinetics (e.g., Evans et al., 2001). Therefore, in our subsequent analysis of the data, we define the starting point for grain growth as the condition where porosity becomes steady state. In the synthetic orthopyroxene, some silica-rich inclusions were found, which resulted from incomplete mixing or non-ideal stochiometry during sample synthesis. The olivine powder, added to the experiments to buffer the oxide activity, was always present after the experiment. The presence of both silica and olivine indicates that equilibrium with respect to the oxide activity was not achieved. The possible consequences of disequilibrium with respect to oxide activity, and the issue of equilibrium with respect to oxygen fugacity will be considered in Section 4.

The results of the grain-growth experiments are summarized in Table 2. In all experiments, substantial grain growth was observed in the synthetic orthopyroxene. From an initial grain size of approximately 1 μm, grains grew to approximately 40 μm after 34 h. In contrast, no perceptible grain growth was observed in the natural orthopyroxene. Data can be fit to a standard grain-growth equation (e.g., Burke, 1966),

$$\bar{d}_{\mathrm{f}}^{n} - \bar{d}_{\mathrm{o}}^{n} = kt \tag{1}$$

$$k = k_{\mathrm{o}} \exp\left(-\frac{H^*}{RT}\right) \tag{2}$$

where d_{f} is the final grain size, d_{o} the initial grain size, k a rate constant that is proportional to grain-boundary mobility, t the time, and n is a constant that should be approximately 2–4, depending on the rate-limiting mechanism (Kingery et al., 1976). Although the natural orthopyroxene in these experiments show no quantifiable grain growth, there is sufficient data on the synthetic orthopyroxene to fit these equations. For the synthetic orthopyroxene the parameter n was determined to be 2.4 ± 0.7 using a non-linear least-squares regression of all of the experimental data at 1573 K (Fig. 5). H^* ($=720 \pm 80$ kJ/mol) and k_{o} ($=10^{8.2\pm2.8}$ m$^{2.4}$/s) were fit using a linear regression on an Arrhenius plot. Errors reported are one standard deviation.

4. Discussion

4.1. Kinetics of chemical equilibrium

Before we interpret the experimental observations on grain growth in orthopyroxene, we need to address the issue of chemical equilibrium within our experiments. During the course of our experimental study, we have recognized that the kinetics of the reactions required to achieve equilibrium with respect to oxygen fugacity and

Table 2
Summary of experiments

Run #	Temperature (K)	Pressure (GPa)	Duration (h)	Orlhopyroxene grain size (μm)			
				Synthetic		Natural	
				Initial	Final	Initial	Final
GA-134	1573	1.5	4	1.0	4.5	2.8	3.3
GA-135	1573	1.5	16	1.0	35.9	2.8	3.9
GA-136	1573	1.5	10	1.0	20.0	2.8	3.3
GA-137	1573	1.5	8	1.0	19.6	2.8	3.5
GA-141	1573	1.5	32	1.0	34.5	2.8	3.9
GA-159[a]	1573	1.5	34	1.0	41.3	2.8	3.5
GA-169	1523	1.5	10	1.0	7.9	2.8	3.1
GA-148	1473	1.5	12	0.8	5.9	3.0	3.7
GA-152	1473	1.5	30	0.8	6.7	3.0	3.5

[a] Product of two runs—the starting material for this experiment was GA-135.

oxide activity in orthopyroxene are considerably more sluggish than those in olivine.

In several preliminary experiments in a Kawai-type multi-anvil apparatus synthetic orthopyroxene powder was isostatically hot-pressed at 1273 or 1473 K from 1 to 9 h. The powders were contained in a nickel foil capsule that was intended to set the f_{O_2} at the Ni–NiO buffer. The powder used as the starting material for these experiments had been dried in air for 24 h at 873 K and was somewhat oxidized (as evidenced by the change in color from white to light brown after drying). After the hot-press experiments, the orthopyroxene immediately adjacent to the capsule was optically clear, suggesting local equilibration with the capsule was achieved. However, the orthopyroxene in the center of the capsule was apparently highly oxidized, containing submicron reddish precipitates (likely hematite), suggesting that equilibrium was incomplete. Two experiments at the same temperature, run for 1 and 9 h, showed that the width of the equilibrated region increased with the square root of time, indicating that the equilibration was diffusion controlled. From $D \sim l^2/t$, we find that the diffusivity of the rate-limiting species is about 10^{-11} m^2/s at 1473 K and 10^{-12} m^2/s at 1273 K. This is roughly two orders of magnitude slower than the rate of equilibration for olivine at the same temperatures (Karato and Sato, 1982). The samples used in the grain-growth experiments were less than 0.5 mm thick; equilibration with respect to f_{O_2} should have occurred during the first hour of the experiment.

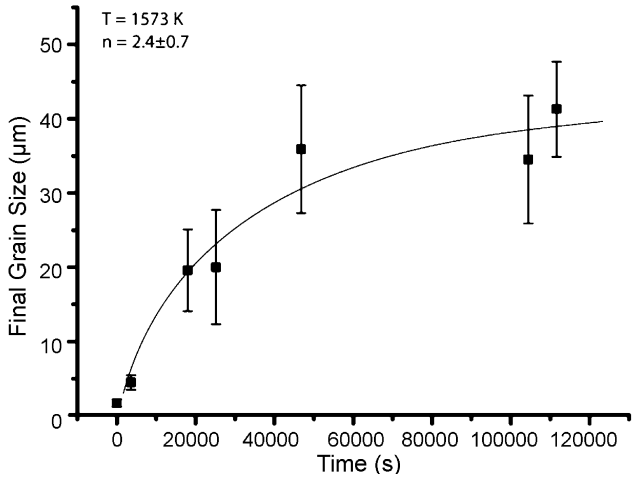

Fig. 5. Synthetic orthopyroxene data at 1573 K. The final grain size is plotted against the duration of the experiment. n is fit using a non-linear least-squares regression of Eq. (1). Error bars are 1σ.

As noted earlier, even after the longest grain-growth experiments, we found silica inclusions in the synthetic orthopyroxene, indicating that the sample was not in equilibrium with the surrounding olivine buffer. Some of these silica inclusions could be found within a few microns of the olivine, indicating that the diffusive process that controls equilibration with respect to oxide activity is extremely slow (<10^{-16} m^2/s at 1573 K). This is quite different from what is observed in olivine, in which equilibration with respect to oxide activity occurs very quickly ($\sim 10^{-10}$ m^2/s at 1573 K, Mackwell et al., 1988). In order to evaluate the degree to which disequilibrium with respect to oxide activity may influence the results on grain-growth kinetics, let us evaluate the difference in oxide activity corresponding to the end-member situations. In our experiments, two end-member cases can be considered: excess MgO (Eq. (3)) and excess SiO_2 (Eq. (4)).

$$MgSiO_3 + MgO \Leftrightarrow Mg_2SiO_4 \quad (3)$$

$$MgO + SiO_2 \Leftrightarrow MgSiO_3 \quad (4)$$

The natural orthopyroxene was equilibrated in Earth in the presence of olivine; with both olivine and orthopyroxene phases present, the MgO activity will be defined by the reaction in Eq. (3). The synthetic orthopyroxene was prepared in the presence of excess SiO_2; with both silica and orthopyroxene phases present, the MgO activity will be defined by the reaction in Eq. (4). Applying the thermodynamic data of Robie et al. (1978), the difference in the magnitude of a_{MgO} for these two end-member cases is a factor of ~1.8. To interpret our data, we would like to know whether the observed contrast in grain growth between the natural and synthetic orthopyroxene may be solely attributable to this difference in MgO activity. The effect of the MgO activity on the kinetics of grain growth depends on the specific point defects involved in the rate-limiting process. The specific point defects are unknown, but the largest effect on the rate of grain growth would occur if the movement of V_{Si}'''' or $Si_I^{\bullet\bullet\bullet\bullet}$ controlled grain growth. In these cases, the rate constant k would vary with the MgO activity to the 10/3 or −10/3 power, respectively (Karato, 1974; Stocker and Smyth, 1978). Thus, the variation in the MgO activity between the natural and synthetic orthopyroxene can account for less than one order of magnitude contrast in the rate of grain growth. Therefore, we conclude that the observed contrast between the natural and synthetic orthopyroxene cannot be solely attributable to differences in oxide activity.

4.2. Interpretation of the experimental data on grain growth

Theory predicts that for normal grain growth, n should equal 2–3 (Atkinson, 1988). For the synthetic orthopyroxene we determine an n of 2.4 ± 0.7, consistent with this prediction. If we assume for the subsequent discussion that n equals 2, the rate-constant k, for grain growth in synthetic orthopyroxene, is approximately $10^{-14.0}$ and $10^{-15.3}$ m^2/s at 1573 and 1473 K, respectively. These data at 1573 K are very similar to values determined for natural olivine under dry conditions (Karato, 1989) (Fig. 6). In the absence of other grain-size altering processes, these rate constants predict that grains should grow to sizes of the order tens of centimeters over a million years.

The kinetics of grain growth in natural orthopyroxene are not well constrained due to the lack of perceptible grain growth in our experiments. If we assume that Eq. (1) holds for the natural orthopyroxene, these experiments allow us to determine an upper bound for grain-growth kinetics of natural orthopyroxene. The initial grain size of the natural orthopyroxene

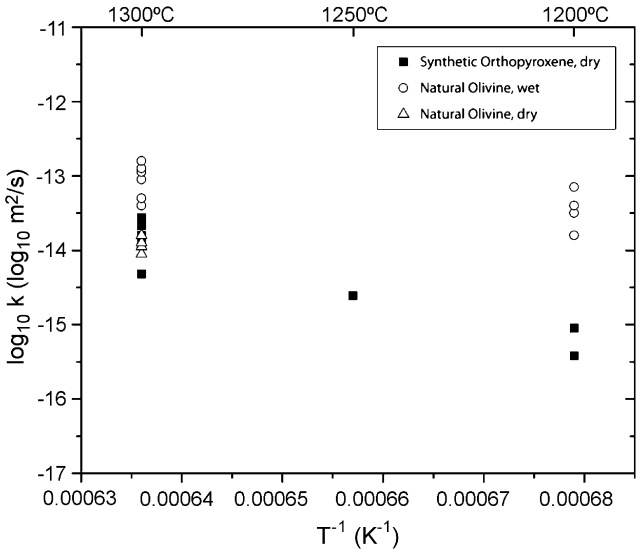

Fig. 6. Kinetics of grain growth in orthopyroxene (this study) and olivine (Karato, 1989), assuming $n = 2$. At 1573 K, under dry conditions, grain-growth kinetics in natural olivine and synthetic orthopyroxene are very similar.

was approximately 3 μm. Roughly speaking, a 50% increase in grain size is needed to be detectable beyond the margins of error. The longest experiment run at the highest temperature (1573 K) was 34 h. If we assume $n = 2$, solving Eq. (1) indicates that for natural orthopyroxene at 1573 K, k must be less than $10^{-16.0}$ m^2/s. This upper bound is two orders of magnitude slower than what was determined for synthetic orthopyroxene; two orders of magnitude is thus a minimum contrast in growth rates between natural and synthetic orthopyroxene at these experimental conditions.

A similar analysis can be made using observations from the deep mantle xenoliths described earlier. In the xenolith samples we have determined from a number of microstructural observations that the orthopyroxene has been recrystallized throughout its deformation history. While there is a clear microstructural relationship between the oldest and newest recrystallized grains, no perceptible growth has occurred in the older recrystallized grains. Both groups of grains have a mean grain size of approximately 35μm. To estimate the duration of deformation, we require an estimate of strain ε and strain-rate $\dot{\varepsilon}$,

$$\tau = \frac{\varepsilon}{\dot{\varepsilon}} \tag{5}$$

A flow law for orthopyroxene in diffusion creep was calculated by reinterpreting the low-stress rheological data from Lawlis (1998). We use the equilibrium temperature (1623 K) and pressure (5.5 GPa) as the conditions of deformation (Boyd, personal communication, 2001).

The stress applied during deformation (~25 MPa) is estimated from the olivine recrystallized grain size and the olivine dislocation density (Karato et al., 1980; Karato and Jung, 2003). Using these parameters, we estimate the strain-rate to be $10^{-10\pm1}\,s^{-1}$. Strain was estimated from the change in shape of the initially equant orthopyroxene porphyroclasts (Boullier and Gueguen, 1975). Finite strains are difficult to constrain because the recrystallized bands of orthopyroxene frequently exceed the length of the thin section and often intersect with other recrystallizing bands. However we conservatively estimate that strain may range from as little as $\varepsilon = 1$ to >100. Using these data, we estimate that recrystallization occurred over $\tau \sim 10^{11\pm2}$ s. Applying the criterion we used earlier for the detectability of grain growth, we find that for the orthopyroxene in these xenoliths k must be less than $10^{-20\pm2}\,m^2/s$, at the conditions of deformation. While inferring material properties from naturally deformed rocks is useful, it is also subject to considerable uncertainties; this analysis should be considered with these uncertainties in mind.

It is well known that in many ceramics the presence of dissolved cations inhibits grain growth (e.g., Yan et al., 1977; Chen and Xue, 1990). Similar observations have been made for halite (Guillopé and Poirier, 1979), olivine (Toriumi, 1982), and calcite (Covey-Crump, 1997). One of the major differences between orthopyroxene and olivine is their capacity to dissolve "impurities". A typical olivine will contain less than 1% impurities (as oxides, by weight, Frey and Prinz, 1978). However, orthopyroxene, depending on temperature and pressure, may dissolve several weight percent impurities (typically Al_2O_3, CaO, and Cr_2O_3). These impurities tend to preferentially segregate into grain-boundaries and near-grain-boundary regions (e.g., Yan et al., 1983; Hiraga et al., 2004). If the lattice diffusion of these impurities is slower than the velocity of the grain boundary, the distribution of ions across the grain boundary will become asymmetric (Toriumi, 1982). The interaction between these ions and the grain boundary will resist the subsequent motion of the grain boundary. In this "loaded" state the grain-boundary mobility will be limited by the lattice diffusivity of the dissolved ions (Yan et al., 1977). Therefore, one possible explanation for the large contrast in grain-growth kinetics between natural orthopyroxene and synthetic orthopyroxene is the reduction of grain-boundary mobility by the grain-boundary segregation of dissolved cations in the natural orthopyroxene. To detect the presence and distribution of these cations in our experimental samples we used high-resolution X-ray mapping on a field-emission gun electron microprobe (FEG-EPMA). These analyses were done with an accelerating voltage of 8 kV, a beam current of 50 nA, and a 40 ns collection time. The results are shown in Fig. 7. We found that the grain-boundary regions in the natural orthopyroxene are enriched in aluminum and calcium, and somewhat depleted in magnesium. The synthetic orthopyroxene was also analyzed, but did not show any grain-boundary segregation. The spatial resolution at these analytical conditions is likely better than 0.5 μm, so the diffuse nature of the grain-boundary segregation is largely an artifact of the limited spatial resolution. The dissolved cations in the natural orthopyroxene do not appear to be uniformly distributed along all grain boundaries. This may indicate that chemical equilibrium was not achieved, or may also be a consequence of the spatial resolution of this analytical technique.

The hypothesis of impurity-controlled grain growth in natural orthopyroxene can be evaluated using a theoretical model. When grain-boundary mobility is limited by solute drag, mobility can be approximated by (Yan et al., 1977),

$$M(T) \cong \frac{\Omega}{kT}\frac{D_s(T)}{2\delta C_\infty \exp(Q/RT)} \tag{6}$$

where Ω is the ionic volume, D_s the diffusivity of the rate-limiting solute ion, 2δ the width of the region of the solute segregation, C_∞ the concentration of the solute ion far from the grain boundary, and Q is the interaction energy between the solute ion and the grain boundary.

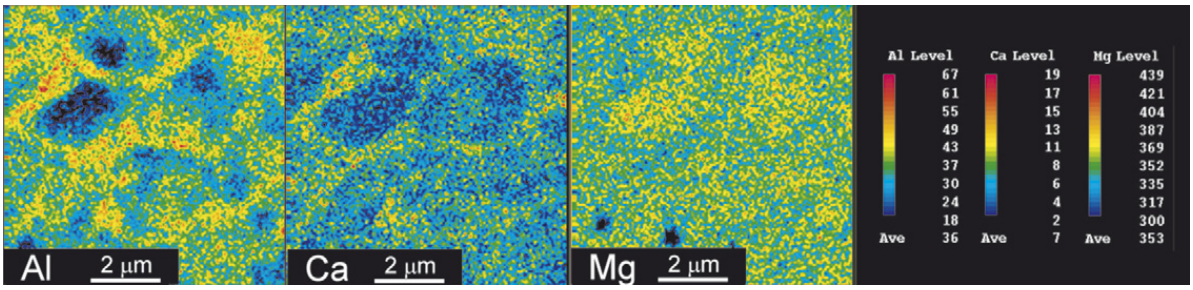

Fig. 7. X-ray maps of aluminum, calcium and magnesium, in the natural orthopyroxene. Aluminum and calcium are enriched along grain boundaries, while magnesium is slightly depleted.

M is related to k by,

$$k = A\gamma M \tag{7}$$

where A is a non-dimensional constant of order ~0.5 (Hillert, 1965) and γ is the grain-boundary energy (~1 J/m^2, Cooper and Kohlstedt, 1982). There is limited data on diffusion in orthopyroxene, so for this calculation we assume that calcium is the rate-limiting solute cation. The lattice diffusivity of calcium in orthopyroxene is 10^{-16} m^2/s at 1573 K (Huebner and Voigt, 1984). The width of the region of solute segregation is not well constrained, but is thought to be of the order of ~10 nm (Kingery, 1974a,b). The concentration of calcium in the matrix was determined by microprobe analysis (Table 1). When the interaction between the impurity atoms and the matrix is mostly elastic, the interaction energy can be written as (Yan et al., 1977),

$$Q = \frac{4\pi r^3 E}{(1+\nu)}\left(\frac{\Delta r}{r}\right)^2 \tag{8}$$

where r is the radius of the matrix ion, E the Young's modulus, ν the Poisson's ratio, and Δr is the size difference between the solute ion and the matrix ion, which in this case is the difference in ionic radius between Ca^{2+} and Mg^{2+}. From Eq. (8) we estimate the interaction energy to be ~80 kJ/mol. Using Eqs. (6)–(8), we calculate the rate constant k to be ~10^{-19} m^2/s at 1573 K (for simplicity we have ignored the effects of pressure). This rate of grain growth predicts that grains should only grow to 2 mm over a million years. We understand that this is a very crude estimate of grain-boundary mobility, but the result is in agreement with our experimental observations, which indicate that k for the natural orthopyroxene must be less than ~10^{-16} m^2/s at 1573 K.

4.3. Implications for upper mantle rheology and shear localization

Although grain size may influence a number of geological phenomena, a topic of particular interest has been the process of grain-size reduction induced weakening (e.g., Rutter and Brodie, 1988). During this process, grain-size reduction by dynamic recrystallization leads to a transition from dislocation creep to diffusion creep. Because diffusion creep is highly grain-size sensitive, this transition will result in a reduction in viscosity. This has been recognized as a potentially important mechanism for weakening the lithosphere (Bercovici and Karato, 2002; Bercovici, 2003). However, grain-size reduction induced weakening can only be a transient phenomenon, because after the cessation of dislocation creep, grains will begin to grow, and the deforming material will strengthen. In order for grain-size reduction induced weakening to be geologically significant, the time scale for grain growth must be much longer than the time scale for deformation. A recent study by Warren and Hirth (2006) has argued that pinning by secondary phases provides a mechanism for inhibiting grain growth, thus permitting long-term weakening. However, this particular model requires at least two minerals to recrystallize and become intimately mixed by grain-boundary sliding processes. In our study, we have demonstrated that grain growth in orthopyroxene may be inhibited simply by the equilibrium segregation of solute ions on and near grain boundaries.

As noted earlier, the difference in the behavior of orthopyroxene and olivine is partially a consequence of the differences in their capacity to dissolve impurities. A further complication is that in orthopyroxene, the concentrations of these impurities vary strongly as a function of pressure, temperature, and lithology (e.g., Brey et al., 1990). This compositional variability creates a strong extrinsic pressure and temperature dependence to the kinetics of grain growth. The pressure and temperature dependence of grain growth is further modified by the activation enthalpy of diffusion of the rate-limiting solute cation, and the energy of interaction between this cation and the grain boundary. In summary, the inhibition of grain growth, and consequent viability of grain-size reduction induced weakening will vary as a particularly complicated function of temperature and pressure. Further research on the diffusivity of aluminum, calcium, and chromium in orthopyroxene, coupled with an improved understanding of the distribution of these cations around grain boundaries, will provide great insights into the nature of grain growth and thus deformation processes in the upper mantle.

5. Conclusions

We have conducted a series of experiments on the kinetics of grain growth in natural and synthetic orthopyroxene, within the orthoenstatite stability field. In these experiments, the grain size of synthetic orthopyroxene increases markedly, while natural orthopyroxene shows no perceptible growth. The kinetics of grain growth in the synthetic orthopyroxene are similar to the kinetics of grain growth in natural olivine (Karato, 1989), however the kinetics of grain growth in natural orthopyroxene are at least two orders of magnitude slower. The difference in this behavior is attributed to the presence of dissolved cations such as aluminum and calcium, which have been segregated to the grain boundaries. A high-resolution microprobe study supports this conclu-

sion. Slow grain-growth kinetics in orthopyroxene may provide a mechanism for the long-term weakening of deformed and recrystallized peridotitic rocks.

Acknowledgements

We thank Dr. Masaru Takakura at JEOL-Japan for his assistance with the high-resolution FEG-EPMA composition measurements. Dr. Tomoaki Kubo and an anonymous reviewer are thanked for their helpful comments on the manuscript. This research was supported by an MSA Grant for Student Research and NSF EAR-0309448.

References

Atkinson, H., 1988. Theories of normal grain growth in pure single phase systems. Acta Metall. 36 (3), 469–491.

Bercovici, D., Karato, S-i., 2002. Theoretical analysis of shear localization in the lithosphere. In: Karato, S-i., Wenk, H.R. (Eds.), Plastic Deformation of Minerals and Rocks. Mineralogical Society of America and Geochemical Society, Washington, DC, United States.

Bercovici, D., 2003. The generation of plate tectonics from mantle convection. Earth Planet. Sci. Lett. 205 (3/4), 107–121.

Boullier, A.M., Gueguen, Y., 1975. SP-mylonites; origin of some mylonites by superplastic flow. Contrib. Mineral. Petrol. 50 (2), 93–104.

Brey, G.P., Koehler, T., Nickel, K.G., 1990. Geothermobarometry in four-phase lherzolites. I: Experimental results from 10 to 60 kb. J. Petrol. 31 (6), 1313–1352.

Burke, J.E., 1966. Grain growth. In: Fulrath, R., Pask, J.A. (Eds.), Ceramic Microstructures. Robert E. Krieger Publishing, pp. 681–700.

Chen, I., Xue, L., 1990. Development of superplastic structural ceramics. J. Am. Ceram. Soc. 73, 2585–2609.

Cooper, R.F., Kohlstedt, D.L., 1982. Interfacial energies in the olivine-basalt system. In: Akimoto, S., Manghnani, M.H. (Eds.), High Pressure Research In Geophysics. Advances in Earth and Planetary Sciences (AEPS). Center for Academic Publications Japan, Tokyo, Japan, pp. 217–228.

Covey-Crump, S.J., 1997. The normal grain growth behaviour of nominally pure calcitic aggregates. Contrib. Mineral. Petrol. 129 (2–3), 239–254.

de Bresser, J.H.P., Peach, C.J., Reijs, J.P.J., Spiers, C.J., 1998. On dynamic recrystallization during solid state flow; effects of stress and temperature. Geophys. Res. Lett. 25 (18), 3457–3460.

de Bresser, J.H.P., Ter Heege, J.H., Spiers, C.J., 2001. Grain size reduction by dynamic recrystallization; can it result in major rheological weakening? In: Dresen, G., Handy, M. (Eds.), Deformation Mechanisms, Rheology and Microstructures. Springer International, Berlin, Federal Republic of Germany, p. 2001.

Dresen, G., Wang, Z., Bai, Q., 1996. Kinetics of grain growth in anorthite. Tectonophysics 258 (1–4), 251–262.

Evans, B., Renner, J., Hirth, G., 2001. A few remarks on the kinetics of static grain growth in rocks. In: Dresen, G., Handy, M. (Eds.), Deformation Mechanisms, Rheology and Microstructures. Springer International, Berlin, Federal Republic of Germany, p. 2001.

Frey, F.A., Prinz, M., 1978. Ultramafic inclusions from San Carlos, Arizona; petrologic and geochemical data bearing on their petrogenesis. Earth Planet. Sci. Lett. 38 (1), 129–176.

Guillopé, M., Poirier, J.P., 1979. Dynamic recrystallization during creep of single-crystalline halite; an experimental study. J. Geophys. Res. 84 (B10), 5557–5567.

Handy, M.R., 1994. Flow laws for rocks containing two non-linear viscous phases; a phenomenological approach. J. Struct. Geol. 16 (3), 287–301.

Hillert, M., 1965. On the theory of normal and abnormal grain growth. Acta Metall. 13, 227–238.

Hiraga, T., Anderson, I.M., Kohlstedt, D.L., 2004. Grain boundaries as reservoirs of incompatible elements in the Earth's mantle. Nature (London) 427 (6976), 699–703.

Huebner, J.S., Voigt, D.E., 1984. Chemical diffusion in Ca–Mg–Fe pyroxenes; measured rates of cation exchange and interface movement. In: The Geological Society of America, 97th Meeting. Abstracts with Programs—Geological Society of America, Geological Society of America (GSA), Boulder, CO, United States, p. 546.

Karato, S-i., 1974. Lattice defects and transport properties of olivine. M.Sc. Thesis, University of Tokyo, 30 pp.

Karato, S-i., Toriumi, M., Fujii, T., 1980. Dynamic recrystallization of olivine single crystals during high-temperature creep. Geophys. Res. Lett. 7 (9), 649–652.

Karato, S-i., Sato, H., 1982. Effect of oxygen partial pressure on the dislocation recovery in olivine; a new constraint on creep mechanisms. Phys. Earth Planet. Interiors 28 (4), 312–319.

Karato, S-i., 1989. Grain growth kinetics in olivine aggregates. Tectonophysics 168 (4), 255–273.

Karato, S-i., Wu, P., 1993. Rheology of the Upper Mantle: A synthesis. Science 260, 771–777.

Karato, S-i., Jung, H., 2003. Effects of pressure on high-temperature dislocation creep in olivine. Philos. Mag. 83 (3), 401–414.

Kingery, W., 1974a. Plausible concepts necessary and sufficient for interpretation of ceramic grain-boundary phenomena. I: Grain boundary characteristics, structure, and electrostatic potential. J. Am. Ceram. Soc. 57 (1), 1–8.

Kingery, W., 1974b. Plausible concepts necessary and sufficient for interpretation of ceramic grain-boundary phenomena. II: Solute segregation, grain-boundary diffusion, and general discussion. J. Am. Ceram. Soc. 57 (2), 74–83.

Kingery, W., Bowen, H., Uhlmann, D., 1976. Introduction to Ceramics. John Wiley and Sons, 1032 pp.

Lawlis, J., 1998. High temperature creep of synthetic olivine-enstatite aggregates. Doctoral Thesis, Pennsylvania State University, 132 pp.

Mackwell, S., Dimos, D., Kohlstedt, D., 1988. Transient creep of olivine: point-defect relaxation times. Philos. Mag. A 57 (5), 779–789.

Mirwald, P., Getting, I., Kennedy, G., 1975. Low-friction cell for piston-cylinder high-pressure apparatus. J. Geophys. Res. 80, 1519–1525.

Nishihara, Y., Shinmei, T., Karato, S-i., 2006. Grain-growth kinetics in wadsleyite: effects of chemical environment. Phys. Earth Planet. Interiors 154, 30–43.

Paterson, M.S., 1982. The determination of hydroxyl by infrared absorption in quartz, silicate glasses and similar materials. Bull. Miner. 105 (1), 20–29.

Presnall, D., 1995. Phase diagrams of Earth-forming minerals. In: Ahrens, T. (Ed.), Mineral Physics and Crystallography: A Handbook of Physical Constants. American Geopysical Union.

Robie, R., Hemingway, B., Fisher, J., 1978. Thermodynamic properties of minerals and related substances at 298.15 K and 1 bar (10^5 Pascal) pressure and at higher temperatures. US Geological Survey Bulletin, p. 1452.

Rutter, E.H., Brodie, K.H., 1988. The role of tectonic grain size reduction in the rheological stratification of the lithosphere. In: Zankl, H., Belliere, J., Prashnowsky, A. (Eds.), Detachment and Shear. Geologische Rundschau. Springer International, Berlin, Federal Republic of Germany, pp. 295–308.

Stocker, R.L., Smyth, D.M., 1978. Effect of enstatite activity and oxygen partial pressure on the point-defect chemistry of olivine. Phys. Earth Planet. Interiors 16 (2), 145–156.

Toriumi, M., 1982. Grain boundary migration in olivine at atmospheric pressure. Phys. Earth Planet. Interiors 30 (1), 26–35.

Tullis, J., Yund, R.A., 1982. Grain growth kinetics of quartz and calcite aggregates. J. Geol. 90 (3), 301–318.

Underwood, E., 1970. Quantitative Stereology. Addison Wesley Publishing Company, 274 pp.

Warren, J., Hirth, G., 2006. Grain size sensitive deformation mechanisms in naturally deformed peridotites. Earth Planet. Sci. Lett. 248, 438–450.

Yan, M., Cannon, R.M., Bowen, H.K., 1977. Grain boundary migration in ceramics. In: Fulrath, R., Pask, J.A. (Eds.), Ceramic Microstructures. Westview Press, pp. 276–307.

Yan, M., Cannon, R., Bowen, H., 1983. Space-charge, elastic field, and dipole contributions to equilibrium solute segregation at interfaces. J. Appl. Phys. 54, 764–778.